JOURNAL OF CATALYSIS **167,** 408–411 (1997)
ARTICLE NO. CA971587

Effects of Chemisorption on the Surface Composition of Bimetallic Catalysts

Ling Zhu,* Ruoping Wang,* Terry S. King,† and Andrew E. DePristo*,‡

*Ames Laboratory, U.S. Department of Energy, †Department of Chemical Engineering, and ‡Department of Chemistry, Iowa State University, Ames, Iowa 50011

Received June 14, 1996; revised December 13, 1996; accepted December 23, 1996

We have investigated the effect of hydrogen chemisorption on the surface composition of bimetallic RhPt catalytic clusters using the bond order metal simulation model. The differences in adsorption energies of hydrogen on Rh and on Pt for one monolayer of hydrogen are obtained by scaling the values for single-hydrogen adsorption, predicted by non-self-consistent electron density functional theory, until the results for surface segregation data from nuclear magnetic resonance are reproduced. We find the best fit with energy differences of −8.19 and −12.75 kJ/mol for three- and fourfold fcc hollow sites, respectively, in excellent agreement with the recent calorimetric measurements of −6 kJ/mol for the average heat of adsorption. In the presence of hydrogen, our cluster surfaces are Rh-rich, especially for the fcc(100) faces, completely reversing the segregation of Pt to the surface of the bare cluster. © 1997 Academic Press

I. INTRODUCTION

RhPt bimetallic clusters are the prime catalysts for the simultaneous conversion of carbon monoxide, hydrocarbons, and nitrogen oxides in automobile exhaust converters (1–3). This fact has stimulated extensive experimental and theoretical research into specific catalytic properties of these clusters (1–11). Key factors are the geometry and the structure, i.e., the overall cluster shape, as well as details of the segregation of the different species between the bulk and the cluster surface, and their micromixing at the surface. These issues have been addressed theoretically by us in a number of publications, using the bond order metal simulation (BOS) model (12–19), including the previous and following papers in the present series of three.

Recently (17), we have generalized this model to include the variation of the metal–metal bond strength with the number and the type of atomic neighbors, and have demonstrated how to determine model parameters from experimental results (16–18).

Here we include a new feature in the model: chemisorption of nonmetals. This is crucial to understand the behavior of catalytic converters, where active molecules, such as hydrogen, oxygen, and carbon monoxide, may adsorb on the RhPt clusters. Indeed, studies of the $Pt_{0.25}Rh_{0.75}$ (100) surfaces (8) have shown alteration and even reversal of the Pt surface enrichment, due to chemisorption of oxygen.

In the following, we first describe the model and its general implementation. We then apply the model to analyze the effect of hydrogen chemisorption on the Rh_xPt_{1-x} systems.

II. THEORETICAL METHODOLOGY

For simplicity, consider a system of N metal atoms, $\{A_i, i = 1, \ldots, N\}$, of two types ("A" or "B") and N_a single type of adsorbate units, $\{X_j, j = 1, \ldots, N_a\}$. In addition, assume that: (i) the adsorbates can bind only to the surface of the metal cluster; (ii) the adsorbate–metal bond energy is equal to that on a pure metal substrate (of pure A or pure B), at the same adsorption site (this bond energy is then equal to the adsorption energy for the pure metal divided by the total number of metal-adsorbate pairs); and (iii) the adsorbate–metal bonds are sufficiently weak to leave the cluster geometry unchanged.

The above assumptions lead to the following form for the energy of a metal atom, say, A with (Z-M) nearest neighbors of type A, M neighbors of type B, and L adsorbates of type X:

$$\varepsilon^{\mathrm{A}}_{(Z\text{-}M)\text{ of A}+M\text{ of B}+L\text{ of X}} = \varepsilon^{\mathrm{A}}_{Z} + M\Delta E^{\mathrm{A}}_{Z,\,\mathrm{A-B}} + \frac{M(M-1)}{2}\lambda^{\mathrm{A}}_{Z,\,\mathrm{A-B}} + \sum_{j=1}^{L}\frac{\Delta E_{\mathrm{ads}}(X(A),\,j)}{z_j}, \quad [1]$$

where $\varepsilon^{\mathrm{A}}_{Z}$ is the interaction energy for a Z-coordinated A-type atom with all A-type neighbors; $\Delta E^{\mathrm{A}}_{Z,\,\mathrm{A-B}}$ is the energy change of the first A−B bond compared to an A−A bond; $\lambda^{\mathrm{A}}_{Z,\,\mathrm{A-B}}$ is the incremental variation in the A−B bond energy: $\Delta E_{\mathrm{ads}}(\mathrm{X(A)}, j)$ is the adsorption energy of species X at site j, and z_j is the total number of metal–adsorbate nearest neighbor pairs at this site (e.g., 3 for 3-fold and 4 for 4-fold hollow sites). In the absence of an adsorbate, i.e.,

0021-9517/97 $25.00

if $L = 0$, Eq. [1] reduces to the expression used in Refs. (17, 18). A similar equation holds for metal atoms of type B. The total interaction energy is just the sum of the site energies for all the atoms.

III. DETERMINATION OF MODEL PARAMETERS

The original six BOS parameters, $\varepsilon_Z^{\mathrm{A}}$, $\varepsilon_Z^{\mathrm{B}}$, $\Delta E_{Z,\,\mathrm{A-B}}^{\mathrm{A}}$, $\Delta E_{Z,\,\mathrm{B-A}}^{\mathrm{B}}$, $\lambda_{Z,\,\mathrm{A-B}}^{\mathrm{A}}$, and $\lambda_{Z,\,\mathrm{B-A}}^{\mathrm{B}}$, were determined from experimental dimer energies, surface energies, cohesive energies, and bulk mixing energies as a function of composition (16, 18). The values of $\varepsilon_Z^{\mathrm{Rh}}$ (in eV) are -3.42, -3.82, -4.21, -4.60, and -5.75, for $Z = 6$, 7, 8, 9, and 12, respectively. The corresponding values for $\varepsilon_Z^{\mathrm{Pt}}$ (in eV) are -3.58, -3.99, -4.40, -4.80, and -5.84. The mixing parameters (in kJ/mol) are $\Delta E_{12,\,\mathrm{Rh-Pt}}^{\mathrm{Rh}} = -0.70$, $\Delta E_{12,\,\mathrm{Pt-Rh}}^{\mathrm{Pt}} = 0.03$, and $\lambda_{12,\,\mathrm{Rh-Pt}}^{\mathrm{Rh}} = 0 = \lambda_{12,\,\mathrm{Pt-Rh}}^{\mathrm{Pt}}$, yielding a small bulk mixing energy of -2 kJ/mol for $Rh_{0.5}Pt_{0.5}$ (20) and a completely symmetric mixing energy versus composition curve.

Hydrogen atom–metal bond energies for the various surface sites are also required, and these were estimated in a two-stage procedure. First, we calculated the relative equilibrium adsorption energy of a single hydrogen atom on pure Rh and pure Pt using the Corrected Effective Medium theory in its simplest MD/MC-CEM framework (21). The Rh and Pt fcc(111) and/or fcc(100) surfaces are modeled with five atomic layers, each being a square lattice of 13 atoms on a side. The lowest two layers are fixed to mimic the infinite bulk lattice template. On each of the upper three layers, atoms in the middle 9×9 square-cell are allowed to move, but the remaining atoms are fixed. We initially place a hydrogen atom 2.0–3.0 Bohr above a specific surface site near the center of the layer. The whole system, including the metal surface and the hydrogen atom, is then allowed to relax via a quench. This quench is achieved using a molecular-dynamic simulation in a $3N$-dimensional coordinate space (N = number of active atoms). At the end of the quench, the maximum force on any atom is less then 1×10^{-5} eV/Bohr. The energy difference between the above two structures, i.e., the metal surface with and without adsorbed hydrogen, represents the adsorption energy of a hydrogen atom on the metal substrate at the chosen surface site. We find that the adsorption sites for hydrogen on the Rh surface are energetically more favorable than those on Pt. Specifically, the difference between Rh and Pt is -11.70 kJ/mol for threefold hollow site and -18.22 kJ/mol for fourfold hollow site.

Finally, we scaled these data in order to model the corresponding adsorption energy difference values at monolayer hydrogen coverage. We found that -8.19 and -12.75 kJ/mol for three and fourfold hollow sites, respectively, allow matching of ^{1}H nuclear magnetic resonance (NMR) surface segregation results (see also below) at an assumed 1 ML coverage. ^{1}H NMR surface segregation results are unavailable for other coverages and thus scaled H-atom adsorption energies could not be ascertained as a function of coverage at present. Note also that absolute H-atom chemisorption energies are not determined by this procedure, only differences between H–Rh and H–Pt chemisorption energies.

Before presenting detailed simulation results, we describe the controlling factors in a more qualitative manner. For the Rh–Pt system, the surface energy difference, e.g., $(\varepsilon_9^{\mathrm{Pt}} - \varepsilon_{12}^{\mathrm{Pt}}) - (\varepsilon_9^{\mathrm{Rh}} - \varepsilon_{12}^{\mathrm{Rh}})$ for the (111) surface, is much larger than the mixing energy. In the absence of hydrogen, the surface segregation is controlled the surface energy difference, leading to an enrichment of Pt at the surface. The difference in H-atom chemisorption energies is comparable to the surface energy difference in magnitude and reversed in direction, i.e., H–Rh bonds are stronger than H–Pt bonds. Thus, in the presence of hydrogen, the surface segregation can be modified substantially to enrichment of Rh at the surface. The degree of enrichment can be predicted by detailed simulations which we now present.

IV. RESULTS FOR Rh_xPt_{1-x} CLUSTERS

We applied the above model (and parameters) to study the microstructures of Rh_xPt_{1-x} systems with and without adsorbed hydrogen at 304 K. We used a perfect cubo-octahedral shaped metallic cluster of 2406 atoms (which has a 31% dispersion or 752 surface atoms). For this cluster, there are 24, 144, 96, and 488 atoms occupying the 6-coordinated corner, 7-coordinated edge, 8-coordinated fcc(100) site, and 9-coordinated fcc(111) site, respectively. For the hydrogen-covered Rh_xPt_{1-x} system, we introduced a monolayer of hydrogen on the most stable surface sites, i.e., the three- and fourfold hollow sites. Thus, there are 600 and 150 hydrogen atoms occupying three- and fourfold fcc hollow sites, respectively; 10^7 Monte Carlo atomic steps were used to find the equilibrium structures at 304 K. Quantitative analyses were performed every 2×10^5 cycles after an initial 8×10^6 cycles. This was sufficient to obtain convergence of the average values.

In the absence of hydrogen, Rh_xPt_{1-x} clusters with $x =$ 0.1–0.9 form in a very simple manner. The Rh atoms preferentially fill 12-fold coordinated bulk sites, then 9-fold coordinated sites, and so on, until all Rh atoms are used. The Pt atoms then just fill the remaining empty sites, resulting in Pt-rich surface (see Fig. 1a for $x = 0.5$).

In the presence of hydrogen the situation is more complicated. In particular, we find that the participation of hydrogen–metal bonds (with H–Rh favored over H–Pt) can reverse the "preference" for Rh in the filling of the cluster. This reversal leads to Rh-rich surface (see Fig. 1b for $x = 0.5$).

A more quantitative comparison of the clusters in Fig. 1 is provided in Table 1. Consider first the $Rh_{0.5}Pt_{0.5}$ without hydrogen. In this case, the difference in surface energy

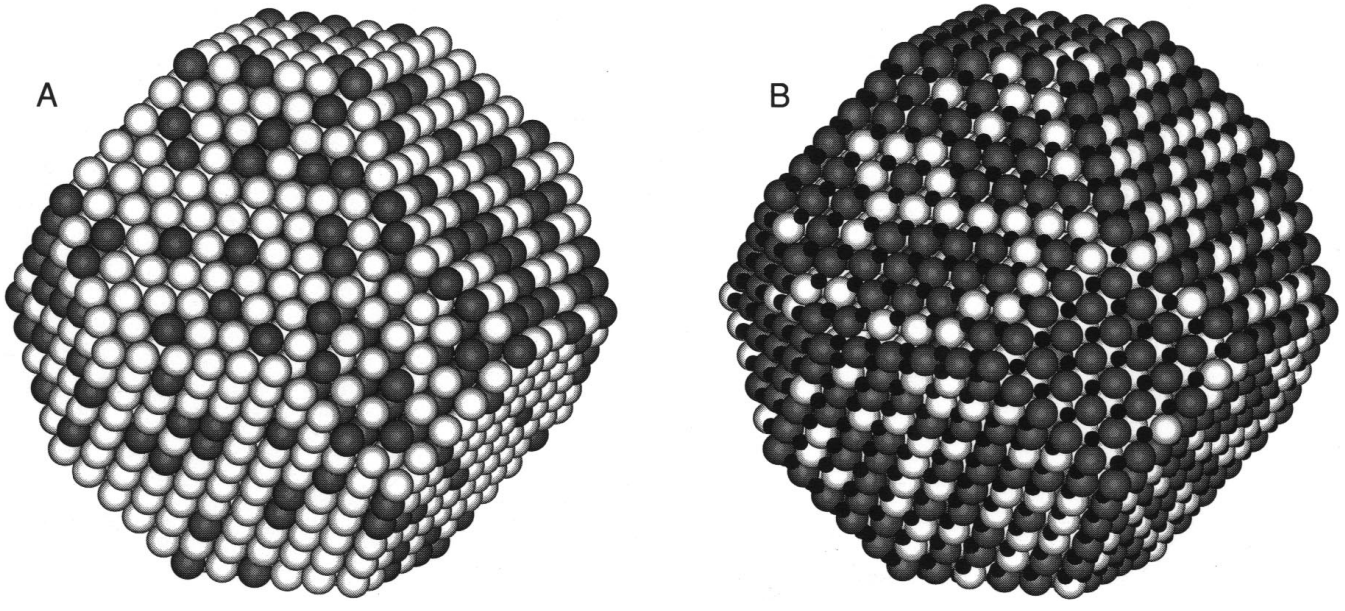

FIG. 1. The structures of $Rh_{0.5}Pt_{0.5}$ clusters at 304 K predicted by the BOS model (a) in the absence of hydrogen and (b) in the presence of hydrogen. Pt atoms are white, Rh atoms are gray, and H atoms are black. Note the effect of hydrogen chemisorption both on the bulk-surface segregation and on the surface microstructure.

drives the segregation of the Pt atoms to the surface. On average, only 45.0% of corner sites, 36.8% of edge sites, 31.8% of fcc(100) sites, and 22.4% of fcc(111) sites are occupied by Rh atoms. The relatively smaller bulk mixing energy and entropy terms influence only the atomic arrangement (or mixing) of Rh and Pt atoms on the surface. Now consider the $Rh_{0.5}Pt_{0.5}$ with a monolayer of hydrogen adatoms. Here, the adsorption energy difference between H−Rh and H−Pt has nearly the same magnitude as the surface energy difference between Rh and Pt. This drives Rh atoms to the surface, especially for fcc(100) sites. The resulting Rh average population of corner, edge, fcc(100), and fcc(111) sites on the cluster surface are 76.7, 75.6, 86.4, and 51.4%, respectively.

V. COMPARISON WITH EXPERIMENT

King *et al.* (22) have used ^{1}H NMR experiments to investigate the overall surface segregation of Rh_xPt_{1-x} clusters, with $x = 0.39$, 0.66, and 0.85, and dispersions of 21–25%, at 304 K. The results showed surface enrichment with Rh atoms in all cases. To fit these data without detailed knowledge of the adsorption energy difference at monolayer coverage of hydrogen, we modeled the energy difference by simply multiplying the values in the limit of zero coverage by a constant, C. The BOS model reproduced all the experimental data with an adsorption energy for $C \approx 0.70$, corresponding to a difference of −8.19 and −12.75 kJ/mol for three- and fourfold hollow sites,

TABLE 1

The Average Percentage of Rh (and Standard Deviations) on Every Site of 2406-Atom $Rh_{0.5}Pt_{0.5}$ Clusters, at 304 K, with and without Adsorbed Hydrogen

Site	σ(Rh, site)-σ(Pt, site)	ΔE_{mix}^{bulk} ($Rh_{0.5}Pt_{0.5}$)	$T\Delta S$ ($Rh_{0.5}Pt_{0.5}$)	ΔE_{ads}(H/Rh, site)-ΔE_{ads}(H/Pt, site)	Rh (%)	
					No H	With H
Corner	6.75	−2	1.8	NA	45.0 ± 8.5	76.7 ± 6.8
Edge	7.72	−2	1.8	NA	36.8 ± 3.6	75.6 ± 2.7
(100)	9.65	−2	1.8	−12.75	31.8 ± 4.2	86.4 ± 2.6
(111)	10.61	−2	1.8	−8.19	22.4 ± 1.2	51.4 ± 1.7
Bulk	NA	−2	1.8	NA	60.4 ± 0.4	44.9 ± 0.5

Note. The BOS-controlling factors (in kJ/mol) include: (i) the difference in surface energy, σ(Rh, site)-σ(Pt, site); (ii) the bulk mixing energy, ΔE_{mix}^{bulk}; (iii) the entropy of mixing for an ideal binary 50%–50% mixture, $T\Delta S$; and (iv) the adsorption energy difference, ΔE_{ads}(H/Rh, site)-ΔE_{ads}(H/Pt, site). NA, not applicable.

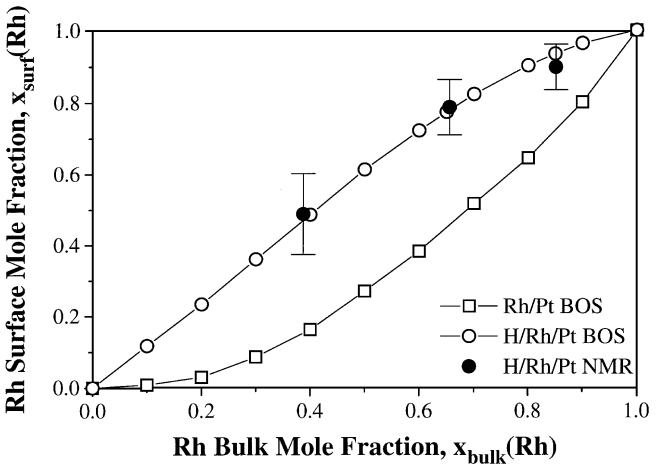

FIG. 2. Surface mole fraction of Rh, x_{surf}(Rh), as a function of the Rh bulk composition, x_{bulk}(Rh), for the 2406-atom Rh_xPt_{1-x} clusters. The BOS predictions for H-covered Rh_xPt_{1-x} clusters compare well with the ^{1}H NMR results. Experimental uncertainties are also shown.

respectively. For comparison, experimental calorimetric measurements (23) yield an average adsorption energy difference of −6 kJ/mol.

Figure 2 shows the variation in Rh surface composition as a function of the Rh bulk composition and chemisorption environment, as predicted by the BOS model and obtained in the experiment. The standard deviations of the BOS simulation results are less than 1%, and therefore are not shown. Note that the results from the BOS simulation agree very well with the ^{1}H NMR results for all three compositions.

VI. CONCLUSIONS

We have applied the bond order metal simulation model to study the microstructures of 2406-atom RhPt catalysts with and without adsorbed hydrogen at 304 K. In the former case, we cover the cluster surface with one monolayer of hydrogen whose adsorption energies are derived from those in the zero-coverage limit. We found that surface segregation is dramatically altered by hydrogen chemisorption. In the absence of hydrogen, the cluster surfaces are Pt-rich. In the presence of hydrogen, the cluster surfaces can be Rh-rich. By adjusting the adsorption energy difference between H on Rh and H on Pt, we have reproduced ^{1}H NMR results for the surface segregation in Rh_xPt_{1-x} clusters for a range of x. The best estimates for the adsorption energy differences used in the simulation agreed well with the calorimetric average.

ACKNOWLEDGMENTS

This work was supported by the Office of Industrial Technology, Energy Efficiency Division, U.S. Department of Energy, through the Ames Laboratory, which is operated for the U.S. Department of Energy by Iowa State University under Contract W-7405-Eng-82.

REFERENCES

1. Taylor, K. C., *Chemtech* **20**, 551 (1990).
2. Taylor, K. C., *Catal. Rev. Sci. Eng.* **35**, 457 (1993).
3. Calvert, J. G., Heywood, J. B., Sawyer, R. F., and Seinfeld, J. H., *Science* **261**, 37 (1993).
4. Oh, S. H., and Carpenter, J. E., *J. Catal.* **98**, 178 (1986).
5. van Langeveld, A. D., and Niemantsverdriet, J. W., *Surf. Sci.* **178**, 880 (1986).
6. van Delft, F. C. M. J. M., van Langeveld, A. D., and Nieuwenhuys, B. E., *Surf. Sci.* **189/190**, 1129 (1987).
7. van Delft, F. C. M. J. M., Siera, J., and Nieuwenbuys, B. E., *Surf. Sci.* **208**, 365 (1989).
8. Yamada, T., Hirano, H., Tanaka, K., Siera, J., and Nieuwenbuys, B. E., *Surf. Sci.* **226**, 1 (1990).
9. Beck, D. D., DiMaggio, C. L., and Fisher, G. B., *Surf. Sci.* **297**, 293 (1993).
10. Ng., K. Y. S., Belton, D. N., Schmieg, S. J., and Fisher, G. B., *J. Catal.* **146**, 394 (1994).
11. Celio, H., and Trenary, M., *J. Phys. Chem*. **99**, 6024 (1995).
12. King, T. S., *in* "Automobile Catalytic Converters" (K. C. Taylor, Ed.). Springer, New York, 1984.
13. Strohl, J. K., and King, T. S., *J. Catal.* **116**, 540 (1989).
14. Strohl, J. K., and King, T. S., *J. Catal.* **118**, 53 (1989).
15. Yang, L., and DePristo, A. E., *J. Catal.* **148**, 575 (1994).
16. Yang, L., and DePristo, A. E., *J. Catal.* **149**, 223 (1994).
17. Zhu, L., and DePristo, A. E., *J. Chem. Phys.* **102**, 5342 (1995).
18. Zhu, L., and DePristo, A. E., *J. Catal.* **167**, 400 (1997).
19. Zhu, L., Liang, K. S., Zhang, B., Bradley, J. S., and DePristo, A. E., *J. Catal.* **167**, 412 (1997).
20. Miedema, A. R., *Philips. Tech. Rev.* **36**, 217 (1976).
21. (a) Raeker, T. J., and DePristo, A. E., *Int. Rev. Phys. Chem*. **10**, 1 (1991). (b) Sinnott, S. B., Stave, M. S., Raeker, T. J., and DePristo, A. E., *Phys. Rev. B* **44**, 8927 (1991). (c) Kelchner, C. L., Halstead, D. M., Perkins, L. S., Wallace, N. M., and DePristo, A. E., *Surf. Sci.* **310**, 425 (1994). (d) DePristo, A. E., *in* "Recent Advances in Density Functional Theory," Vol. 1, Part 1, Chap. 6, "Methodology" (D. Chong, Ed.). World-Scientific, Singapore, 1996.
22. Savargaonkar, N., Pruski, M., and King, T. S., *J. Catal.*, in press.
23. King, T. S. (private communication).